

DSpace Institution

DSpace Repository

<http://dspace.org>

Physics

Thesis and Dissertations

2017-08-04

STUDY OF SUPERCONDUCTIVITY ON NANOSIZE NIOBIUM (Nb)

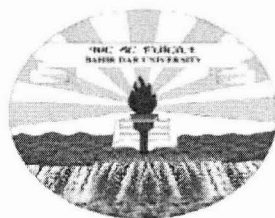
Yilak, Seyoum

<http://hdl.handle.net/123456789/7619>

Downloaded from DSpace Repository, DSpace Institution's institutional repository

STUDY OF SUPERCONDUCTIVITY ON NANOSIZE NIOBIUM (*Nb*)

A THESIS SUBMITTED TO
THE SCHOOL OF GRADUATE STUDIES OF
BAHIR DAR UNIVERSITY



IN PARTIAL FULFILLMENT OF THE
REQUIREMENTS FOR THE DEGREE OF
MASTER OF SCIENCE IN PHYSICS

By

Yilak Seyoum

BAHIR DAR, ETHIOPIA
JUNE 2012



© Copyright by Yilak Seyoum, 2012

BAHIR DAR UNIVERSITY
SCHOOL OF GRADUATE STUDIES


STUDY OF SUPERCONDUCTIVITY ON NANOSIZE
NIOBIUM(Nb)

By

Yilak Seyoum
Department of Physics, College of Science

Approved by the Examining Committee :

Professor P. Singh(External Examiner) 

Dr Getachew Tizazu(Internal Examiner) 

Dr Gebregziabher Kahsay(Advisor) 

BAHIR DAR UNIVERSITY

Date: **June 2012**

Author: **Yilak Seyoum**

Title: **STUDY OF SUPERCONDUCTIVITY ON
NANOSIZE NIOBIUM (*Nb*)**

Department: **Physics**

Degree: **M.Sc.** Convocation: **June** Year: **2012**

Permission is herewith granted to Bahir Dar University to circulate and to have copied for non-commercial purposes, at its discretion, the above title upon the request of individuals or institutions.

Signature of Author

THE AUTHOR RESERVES OTHER PUBLICATION RIGHTS, AND NEITHER THE THESIS NOR EXTENSIVE EXTRACTS FROM IT MAY BE PRINTED OR OTHERWISE REPRODUCED WITHOUT THE AUTHOR'S WRITTEN PERMISSION.

THE AUTHOR ATTESTS THAT PERMISSION HAS BEEN OBTAINED FOR THE USE OF ANY COPYRIGHTED MATERIAL APPEARING IN THIS THESIS (OTHER THAN BRIEF EXCERPTS REQUIRING ONLY PROPER ACKNOWLEDGEMENT IN SCHOLARLY WRITING) AND THAT ALL SUCH USE IS CLEARLY ACKNOWLEDGED.

Dedication

This work is dedicated to my families

Table of Contents

Table of Contents	v
List of Tables	vii
List of Figures	viii
Acknowledgements	x
Abstract	xi
1 General introduction on Superconductivity	1
1.1 Phenomenon of superconductivity: its discovery and evolution	1
1.2 Meissner Effect	4
1.3 Type I and Type II superconductors	5
1.4 The BCS Theory	9
1.5 History of High Temperature Superconductors (Unconventional superconductors)	11
1.6 Application Of Superconductors	12
2 Literature Review	15
2.1 Nanoscience and Nanotechnology	15
2.2 Theoretical overview of Niobium	17
2.2.1 Phonon softening and Transition temperature (T_c) reduction with lattice expansion	20
2.3 Temperature and Energy gap in superconducting Niobium	23
2.4 Superconductivity and Size	26
2.5 Size effects on the normal and superconducting properties of Niobium	27
2.6 Previous studies on nanosize Niobium	30
2.7 Upper critical field in nanostructured Nb	33

3	Mathematical formulation	36
3.1	Transition temperature of strong-coupled superconductors	36
3.1.1	Determination of λ using The phonon frequencies	42
3.2	Ginzburg-Landau Theory, Free energy expansion	43
3.3	Transition temperature and phonon-coupling in Nb	48
3.4	Anderson criteria	50
4	Results and Discussions	52
5	Conclusions and Recommendations	58
	Bibliography	59

List of Tables

List of Figures

1.1	The resistance of mercury sample versus temperature[1]	2
1.2	Evolution of superconductivity over years[2]	3
1.3	Meissner effect[4]	4
1.4	Illustration of superconducting critical surface[5]	5
1.5	Induced magnetic field versus applied magnetic field for type I superconductors[8]	8
1.6	Induced magnetic field versus applied magnetic field for a type II superconductors[8]	8
1.7	Cooper pair[9]	9
1.8	Cooper pair[9]	10
2.1	Crystal structure of Niobium [19]	18
2.2	A summary of various sample parameters for different niobium thin films[20]	21
2.3	Variation of T_c with lattice expansion (Δa)[20]	22
2.4	Energy gap vs temperature for bulk Nb	24
2.5	DOS as a function of energy relative to the Fermi energy at the Fermi level[26]	25
2.6	Variation of H_{C2} with grain size for the nano-Nb[26]	34
4.1	variation of critical temperature with the parameter $(1 + \lambda/\lambda)$ for $\mu^* = 0$	53
4.2	graph of $\ln(\frac{\Theta}{T_c})vs\frac{1+\lambda}{\lambda}$	54
4.3	The parameter γ vs λ graph for $\mu^* = 0.13$	55

4.4 T_c vs λ graph for $\mu^* = 0$ 57

Acknowledgements

First and for most, I would like to thank the almighty God. I would have not been able to carry out this thesis without the help of many people. my special thanks goes to my advisor and instructor, Dr. Gebregziabher Kahsay, for his unlimited and constructive guidance, advice, suggestions and comments through out my work. I would like to forward an exclusive thank to my family for their love, support and constant guidance and care throughout my life. May God bless you two; my mom and dad, as I could never ever thought of any two persons sacrificing and dedicating themselves to my success so trustworthy and humbly. I still have to thank to the rest of my friends, whom I can't name all, but I am sure I owe them a lot for all the good times we have together.

Yilak Seyoum
Bahir Dar, Ethiopia
June, 2012.

Abstract

The main objective of this work is to study the superconductivity of nanosize niobium(Nb). The correlation between the electron-phonon coupling parameter(λ), the Coulomb's pseudopotential(μ^*) and the transition temperature at reduced scales is determined by using the Mcmillan's strong-coupling theory. Using the 'strong coupling theory', the size dependance of the transition temperature of superconducting nanosize Niobium (*Nb*) is derived. The expression for transition temperature has been determined and plotted as a function of the electron-phonon coupling parameter and the Coulomb's pseudopotential for superconducting nanosize Niobium. The dependance of the critical temperature (T_c) with the electron-phonon coupling parameter λ is seen in the graph.

Key words : Mcmillan equation, transition temperature and nanosize Niobium.

Chapter 1

General introduction on Superconductivity

1.1 Phenomenon of superconductivity: its discovery and evolution

The phenomenon of superconductivity, in which the electrical resistance of certain materials completely vanishes at low temperatures, is one of the most interesting and sophisticated phenomena in solid state physics. This phenomena was first discovered by the Dutch physicist Heike Kamerlingh Onnes while studying the resistance of metals at low temperatures in Leiden in 1911 using the recently discovered helium as a refrigerant [1]. He found that, upon cooling the resistance of mercury sample suddenly dropped and it became un detectably small below 4.2K.

Soon after this discovery many other elemental metals were found to exhibit zero resistance when their temperatures were lowered below a certain characteristic temperature of the material, called the critical temperature (T_c). The critical temperature is the temperature at which the phase transition from the normal to the superconducting takes place.

Two years after the discovery of superconductivity in mercury, lead was found to superconduct at 7.2 K. In 1930 superconductivity was discovered in niobium, occurring at a critical temperature of 9.2 K. This is the highest critical temperature among all elemental superconductors. Shortly thereafter the same effect was found in many compounds and alloys when they cooled below certain critical temperatures.

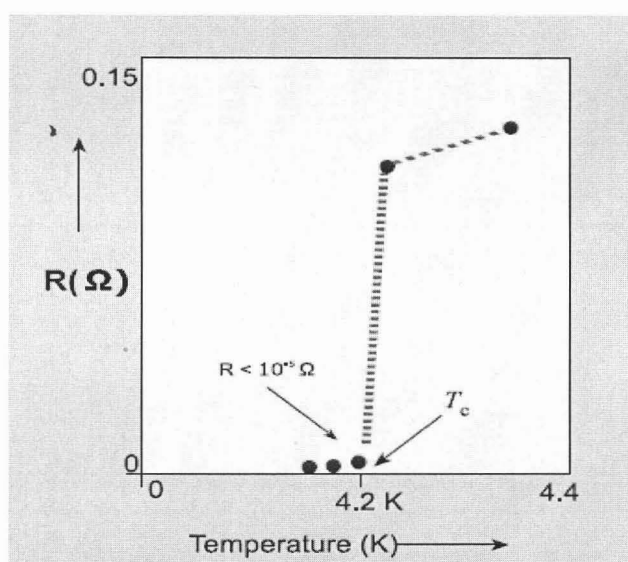


Figure 1.1: The resistance of mercury sample versus temperature[1]

The most surprising thing on superconductivity is that good conductors (such as copper, silver or gold) show no evidence for superconductivity at all. It is still a matter of debate whether or not they would eventually become superconducting if made highly pure and cooled to sufficiently low temperatures.

As recently as 1998, it was discovered that extremely pure platinum becomes superconducting, but only when it is prepared into small nano-particles at temperatures of a few milli Kelvin[2].

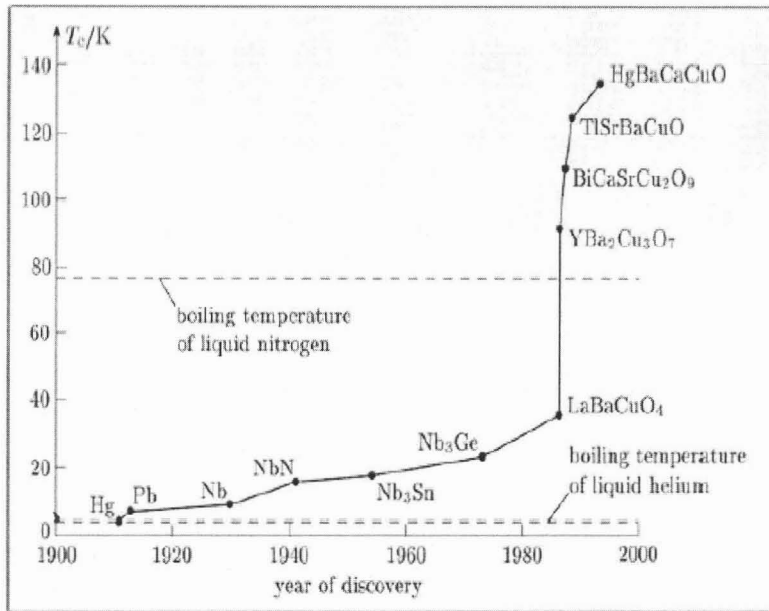


Figure 1.2: Evolution of superconductivity over years[2]

Another recent discovery is that quite a few more elements also become superconducting when they are subjected to extremely high pressures.

Most of the physical properties of superconductors such as critical temperature, critical current density and critical field in which superconductivity is destroyed vary from material to material. However all superconducting materials have zero resistance.

In a normal metal, the current would dissipate due to resistive effects. But Experiments have demonstrated that currents in superconducting coils can persist for years without any measurable degradation because of the absence of resistance with a current lifetime of at least 1×10^5 years[3].

1.2 Meissner Effect

In the year 1933 W. Meissner and his student Robert Ochsenfeld [4] discovered another distinct property of the superconducting state known as perfect diamagnetism while studying the superconducting transition of materials in applied magnetic fields.

They found that a magnetic field was expelled from the interior of the sample (for field up to a critical field H_c), irrespective of the path used to apply the field when the superconductor was cooled in a weak magnetic field below the superconducting transition temperature. This characteristic property of a superconductor is known as the Meissner effect.

The complete expulsion of magnetic field shows that the superconductor is perfectly diamagnetic in the superconducting state. The normal and superconducting state of a material is determined by the temperature, external magnetic field and the current density flowing through the material.

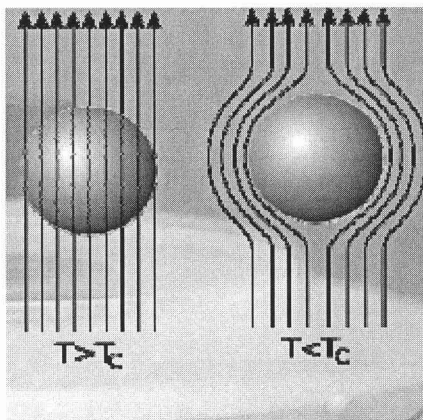


Figure 1.3: Meissner effect[4]

Thus, for the occurrence of superconductivity in a material, the temperature must be below the critical temperature (T_c), the external magnetic field must be below the

critical field (H_c) and the current density flowing through the material must be below the critical current density (J_c). However the behaviour of all superconductors is not the same in this regard and they can be divided into two classes[5] based on the basis of this effect as type I and type II superconductors.

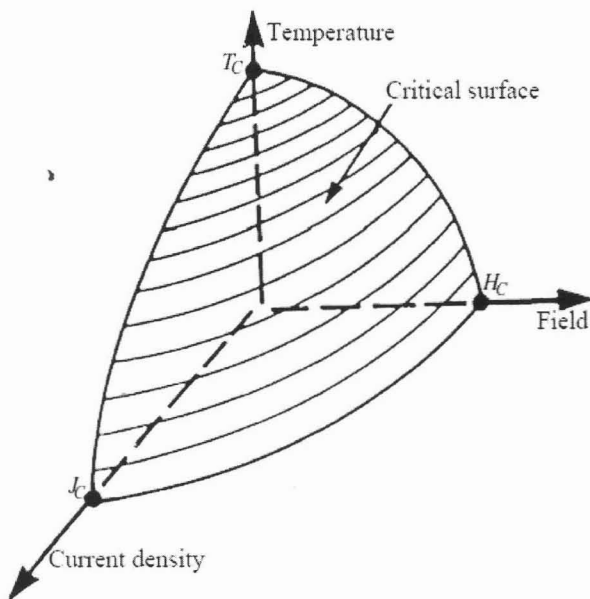


Figure 1.4: Illustration of superconducting critical surface[5]

1.3 Type I and Type II superconductors

It had been thought for many years that all superconductors behaved as those described earlier, exhibiting the Meissner effect in an external magnetic field until superconductivity was destroyed at critical field (H_c). However in 1957, Abrikosov postulated the existence of a different class of superconductor [6], now called type II,

whose behavior in an applied magnetic field differed from conventional expectations. Type I superconductors completely expel the magnetic field until they become completely normal. Above the critical field (H_c), the superconductor is normal and the magnetization (M) = 0.

The normal-superconducting interface contributes a positive energy term. Hence the appearance of normal regions is energetically unfavourable, and the superconductor remains superconducting throughout when a magnetic field of strength less than H_c is applied.

For a type-II superconductor, there are two critical fields; the lower H_{c1} and the upper H_{c2} . The magnetic field completely expelled only up to the lower critical field H_{c1} . Above H_{c1} , the field partially penetrates into the material until upper critical field H_{c2} is reached. Above H_{c2} , the material returns to the normal state. Between H_{c1} and H_{c2} , the material is said to be in mixed(vortex) state. The mixed state is actually caused by vortices in the electronic superfluid, sometimes called fluxons because the field carried by these vortices is quantized. Type II superconductors, however have a negative surface energy term, and as such it is favourable under certain conditions for the superconductor to split into an assemblage of superconducting and normal regions, entering the so-called mixed state[7].

Type-I superconductors include all superconducting elements except few metals like niobium while type-II superconductors include alloys and chemical compounds and some elemental metals, including high T_c superconductors. The value of the ratio of penetration depth to coherence length $\kappa = \frac{\lambda_{GL}}{\xi_{GL}}$ known as the Ginzburg-Landau

parameter distinguishes type I and type II superconductors. For type I superconductors, $\kappa < \frac{1}{\sqrt{2}}$ and for type II superconductors, $\kappa > \frac{1}{\sqrt{2}}$. The negative energy of an interface between normal and superconducting regions in a type II superconductor implies that, under certain conditions of applied magnetic field, it is energetically favourable for the superconductor to subdivide into normal and superconducting regions.

Consequently, a type II superconductor has both a lower and an upper critical fields denoted by H_{c1} and H_{c2} respectively. For fields less than H_{c1} type II superconductors behave in a similar manner to type I superconductors, exhibiting the Meissner effect. However, when the lower critical field is reached, it becomes more energetically favourable to let magnetic field penetrate into the superconductor. This occurs for fields up to H_{c2} (which in fact is equal to $\sqrt{2}\kappa H_c$, and can be much greater than H_c), at which the transition to the normal state occurs.

A type II superconductor can therefore occupy two distinct superconducting states; the Meissner state, in which no magnetic field is present in the interior of the material and the mixed state, where the magnetic field partially penetrates the superconductor.

when an external magnetic field is applied to a Type I superconductor the induced magnetic field exactly cancels that applied field until there is an abrupt change from the superconducting state to the normal state. Type-I superconductors are characterized by a first order phase transition curve $H_c(T)$ from the normal to the superconducting state, with a second order phase transition point at $H_c(T = 0)$.

As noticed earlier, type II superconductors have two critical fields H_{c1} and H_{c2}

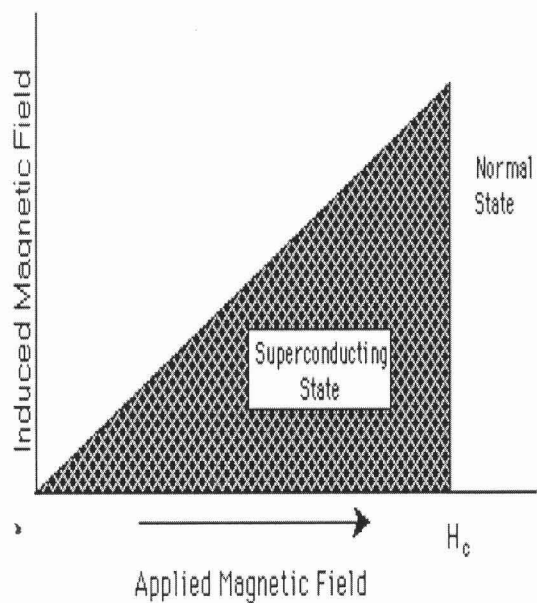


Figure 1.5: Induced magnetic field versus applied magnetic field for type I superconductors[8].

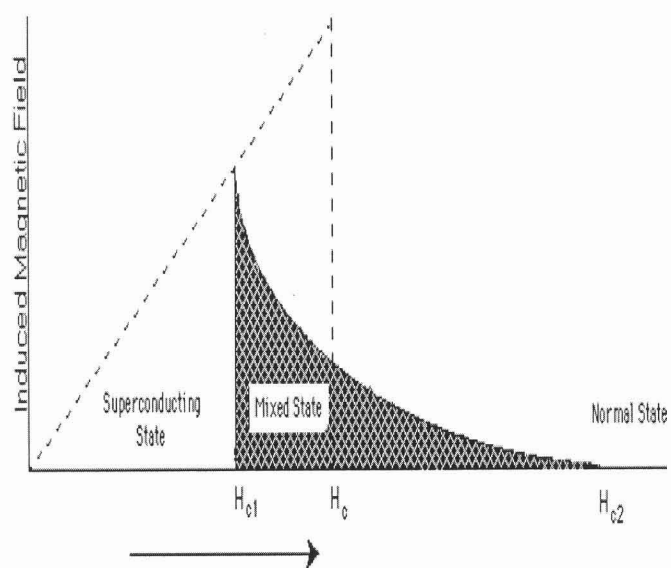


Figure 1.6: Induced magnetic field versus applied magnetic field for a type II superconductors[8].

Below H_{c1} the superconductor excludes all magnetic field lines. At field strengths between H_{c1} and H_{c2} the field begins to intrude in to the mixed state, with some of the material in the normal state and part still in the superconducting state.

1.4 The BCS Theory

A microscopic theory of superconductivity was developed in 1957 by John Bardeen, Leon Cooper and J.Robert Schrieffer which is known as the BCS theory[9]. The central feature of the BCS theory is that two electrons in the superconductor are able to form a bound pair called a Cooper pair if they somehow experience an attractive interaction between them. An electron passes through the lattice and the positive ions are attracted to it, causing a distortion in their nominal positions.

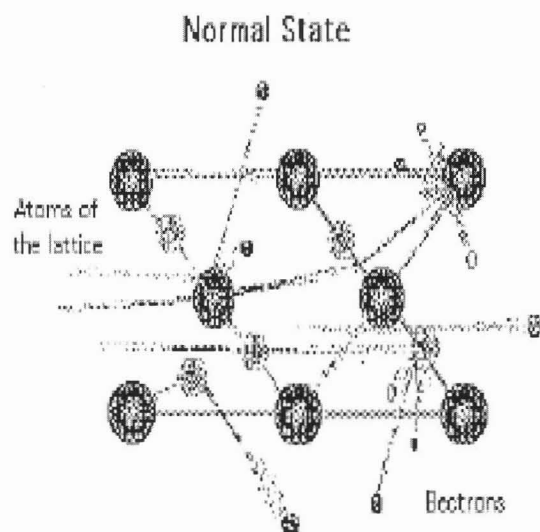


Figure 1.7: Cooper pair[9]

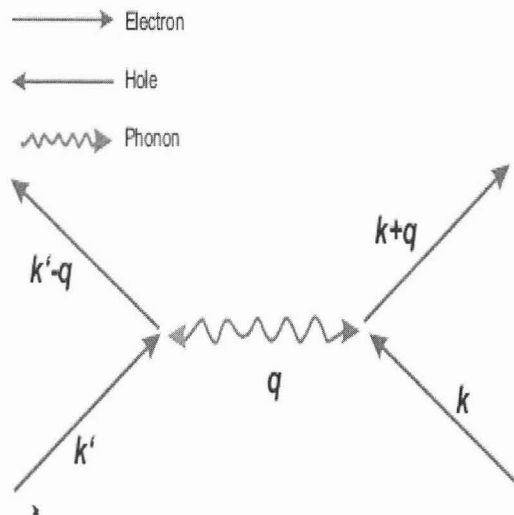


Figure 1.8: Cooper pair[9]

The second electron (the Cooper pair partner) comes along and is attracted by the displaced ions. Note that this second electron can only be attracted to the lattice distortion if it comes close enough before the ions have had a chance to return to their equilibrium positions. The net effect is a weak delayed attractive force between the two electrons.

In the BCS theory, there is interaction of electrons with phonons which produces quantized lattice vibration. An electron moving through the conductor attracts positive ions in the lattice. This attraction can distort the positively charged ions in such a way to attract other electrons (electron phonon interaction). The attraction due to the displaced ion overcomes electron repulsion and causes them to be paired.

The BCS theory describes superconductivity at low temperatures and is subsequently inadequate to explain high temperature superconductivity.

When an electron of a Cooper pair collides with the lattice, it creates a disturbance that is transmitted solely to the other electron in the pair through the crystal lattice. This long range interaction between electrons in the Cooper pairs is because of the conservation of linear momentum.

1.5 History of High Temperature Superconductors (Unconventional superconductors)

The discovery of superconductivity by Kammerling Onnes paved way for condensed matter physicists and material scientists in synthesizing new compounds and discovering this novel phenomenon in a variety of compounds such as pure metals, alloys and mixed oxide systems.

In the late 1986, a major scientific breakthrough occurred in material science. A new class of materials were discovered that displayed superconductivity at unusually high temperatures. The discovery of high temperature superconductivity in a lanthanum-based cuprates by Bednorz and Muller in the year 1986[10] lead to an explosion in research on these materials. The discovery of high-temperature superconductivity in cuprate compounds with layered perovskite structure announced the era of unconventional superconductivity to a wider community. New strategies for the discovery of unconventional superconductors bear fruits besides the tremendous progress in sample production which is a mandatory accessory for the observation of unconventional superconducting phases which are very sensitive to material disorder effects.

Since the discovery of high temperature superconductivity, a large effort has been

made by the scientific community to investigate this field towards a possible application of the new oxide superconductors[11] to different devices like , magnetic bearings, flywheels energy storage, magnetic shielding, transmission cables, fault current limiters, etc. However, all present day large scale applications using superconductivity in accelerator technology are based on conventional materials operating at liquid helium temperatures.

1.6 Application Of Superconductors

Soon after Kamerlingh Onnes discovered superconductivity, scientists began dreaming up practical applications for this strange new phenomenon[12]. Powerful new superconducting magnets could be made much smaller than a resistive magnet, because the windings could carry large currents with no energy loss. Generators wound with superconductors could generate the same amount of electricity with smaller equipment and less energy. Once the electricity was generated it could be distributed and stored for long periods of time without significant loss.

The recent discovery of high temperature superconductors brings us a giant step closer to the dream of early scientists. Applications currently being explored are mostly extensions of current technology used with the low temperature superconductors. Current applications of high temperature superconductors include; magnetic shielding devices, medical imaging systems[13], superconducting quantum interference devices (SQUIDS), infrared sensors, analog signal processing devices, and microwave devices. As our understanding of the properties of superconducting material increases, applications such as; power transmission, superconducting magnets in generators, energy

storage devices, particle accelerators, levitated vehicle transportation, rotating machinery, and magnetic separators will become more practical.

The ability of superconductors to conduct electricity with zero resistance can be exploited in the use of electrical transmission lines. Currently, a substantial fraction of electricity is lost as heat through resistance associated with traditional conductors such as copper or aluminum. A large scale shift to superconductivity technology depends on whether wires can be prepared from the brittle ceramics that retain their superconductivity at 77 K while supporting large current densities.

The field of electronics holds great promise for practical applications of superconductors. The miniaturization and increased speed of computer chips are limited by the generation of heat and the charging time of capacitors due to the resistance of the interconnecting metal films. The use of new superconductive films may result in more densely packed chips which could transmit information more rapidly by several orders of magnitude. Logic delays of 13 picoseconds and switching times of 9 picoseconds have been experimentally demonstrated. Through the use of basic Josephson junctions, scientists are able to make very sensitive microwave detectors, magnetometers, SQUIDs and very stable voltage sources. The use of superconductors for transportation has already been established using liquid helium as a refrigerant. Prototype levitated trains have been constructed in Japan by using superconducting magnets. Superconducting magnets are already crucial components of several technologies. Magnetic resonance imaging (MRI) is playing an ever increasing role in diagnostic medicine. The intense magnetic fields that are needed for these instruments are a perfect application of superconductors. Similarly, particle accelerators used in high-energy physics studies are very dependant on high-field superconducting

magnets.

The recent controversy surrounding the continued funding for the Superconducting Super Collider (SSC) illustrates the political ramifications of the applications of new technologies. New applications of superconductors will increase with critical temperature. Liquid nitrogen based superconductors has provided industry more flexibility to utilize superconductivity as compared to liquid helium superconductors. The possible discovery of room temperature superconductors has the potential to bring superconducting devices into our every-day lives.

High temperature superconducting (HTS) materials have the potential to facilitate a more fundamental change to electric power technologies[14].

Chapter 2

Literature Review

2.1 Nanoscience and Nanotechnology

Nanotechnology is the use of very small particles of material either by themselves or by their manipulation to create new large scale materials[15]. The size of the particles at nanometre scale is 10^{-9} m. The property of materials at nano scale varies from material to material usually in the order of 100 nm or less[16]. Nanotechnology is not a new science and it is not a new technology rather an extension of the sciences and technologies that have already been in development for many years and it is the logical progression of the work that has been done to examine the nature of our world at an ever smaller scale. The size of the particles is the critical factor. At the nanoscale (anything from one hundred or more down to a few nanometres, the properties of materials differ from that of large or bulk scales. As particles become nano-sized, the proportion of atoms on the surface increases relative to those inside and this leads to new properties. It is these nano-effects, however, that ultimately determine all the properties that we are familiar with at our macro-scale and this is where the power

of nanotechnology comes in. If we can manipulate elements at the nanoscale we can affect the macro-properties and produce significantly new materials and processes.

Nanotechnology is an extremely powerful emerging technology, which is expected to have a substantial impact on medical technology now and in the future. The potential impact of novel nanomedical applications on disease diagnosis, therapy and prevention is foreseen to change health care in a fundamental way[17].

Nanotechnology is a ubiquitous technology with a potential impact on every aspect of modern human civilization. It affects an incredibly diverse, such as agriculture, communication, energy generation/transmission, computers, environmental monitoring, food manufacturing/processing, health care, personal care, space travel, robotics, however probably the biggest impact will be in medical technology.

While there are no universally accepted definitions, nanotechnology is generally understood to involve the manipulation of matter on a near-atomic scale to produce new structures, materials, systems, catalysts, and devices that exhibit novel phenomena and properties. Some materials exhibit unique physical, chemical and biological properties at the nanoscale level. Potential benefits result from miniaturization (e.g., sensors) and from the unique properties of the materials (e.g., high strength). Nanotechnology offers the possibility of introducing technologies that are more efficient and environmentally sound than those used today. Nanoscale materials (nanomaterials) contain nanoparticles that are developed using nanotechnology. Nanoparticles are commonly considered to be materials that have at least one dimension which is less than 100 nm. Nanoparticles can occur naturally (e.g., from volcanic eruptions), incidentally (e.g., from fuel combustion); and can be manufactured intentionally. Manufactured nanomaterials can be classified according to their method of production.

Some are produced from the top down, as when a bulk material (e.g., gold, silicate) is reduced to a mass of nanoscale particles. Because of their very small size, these nanoscale metals, metal oxides, powders, and dusts have physical, chemical, magnetic, electrical, mechanical and other properties that differ from those of the bulk materials from which they are derived. The second type of manufactured nanoparticles are built from the bottom up, atom-by atom or molecule-by-molecule. Engineered nanoparticles of this type are still relatively difficult and expensive to manufacture but they have the potential to impact energy development and use, transportation, electronics, manufacturing, and other disciplines.

2.2 Theoretical overview of Niobium

Niobium was discovered by Charles Hatchett in the year 1801 and originally named Columbium. In the following years, it became confused with Tantalum, discovered in 1802, with which it occurs mostly in nature, and was finally isolated and rediscovered in 1844 by Rose and named Niobium. Both names were used until it was officially named Niobium by IUPAC in 1950[18]. However, the name Columbium is still used occasionally by the American metallurgical community.

The superconducting critical temperature T_c of Niobium is known to depend on the density of states $N(E_F)$ at the Fermi energy. This explains the pronounced sensitivity of niobium's critical temperature to crystal lattice imperfections. Niobium is a type II superconductor with transition temperature 9.2K, atomic radius of 0.7\AA . It has the highest transition temperature amongst superconducting elements[19]. It is a transition and a strong-coupled metal characterized by an odd number of protons and an

even number of neutrons in the atomic nucleus. It has 5 valence electrons within the two outer d and s shells with an incomplete d sub-shell[20]. Although the d-shell has higher energy levels, the experimental observations shows that the electrons of the s-shell are removed first.

Nb has body-centered cubic(bcc)crystal structure with $a = b = c = 3.3\text{\AA}$ and $\alpha = \beta = \gamma = 90^\circ$. The fundamental bcc crystal cell has $1 + 8 \times 1/8 = 2$ atoms.

The bond length(x) of transition metals like Niobium represents the shortest atomic

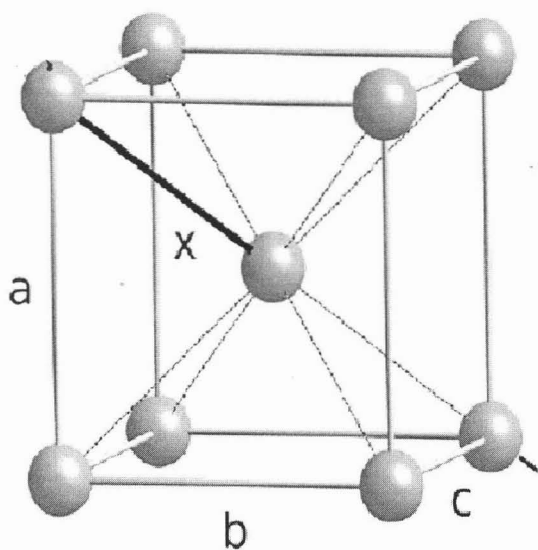


Figure 2.1: Crystal structure of Niobium [19]

separation in a crystal unit cell. It is suggested that there exists a strong correlation between bond length(x) and the inverse of the critical superconducting transition temperature (T_c). The superconducting transition temperature (T_c) is found to decrease monotonically with the increase of the lattice parameter (a) irrespective of its thickness and grain size[20]. The superconducting transition temperature is found to

depend only on the lattice parameter whereas the normal state resistivity depends both on lattice parameter and the details of the sample morphology. Nb thin films show a variation in T_c with varying thickness (t) and grain size (D) or both. According to the BCS theory three parameters, namely density of states (DOS) at Fermi level (E_F), phonon stiffness or Debye temperature (Θ_D) and electronphonon interaction determine T_c . The size dependence of T_c is generally dictated by two effects. The first one is the change in density of states at the fermi level due to energy quantization or due to disorder induced DOS smearing. The second effect is the change in electronphonon interaction arising from surface related effects. However, the same effects reduce the Debye temperature which can in turn reduce T_c . For nano-granular Nb, grain size dependent superconducting properties have been probed by Bose et al[21] who found the relationship between a decrease in T_c and BCS gap $\Delta(0)$ with reduction in grain size which is consistent with the BCS relation.

The Reduction in the Debye temperature (Θ_D) with lattice expansion (Δa) has been observed for a number of nano-composite materials and in particular for Nb. A size dependent change in T_c was observed in terms of reduction in Debye temperature Θ_D due to surface effects. A significant increase in the lattice parameter with the increase of the disorder was also observed in some other experiments on the disordered Nb. There also be observed an other lattice parameter, thickness (t) which affect the value of in T_c in nano size materials.

Recently, it is reported that nano Nb exhibit a systematic lattice expansion as thickness(t) and particle size (D) are reduced. Nano Nb thin films show a systematic lattice expansion with decreasing grain size. The T_c of these films were also decreased

systematically with decreasing grain size. When the lattice parameter change by controlling both t and D , there exists a monotonic decrease and increase in transition temperature (T_c). This decrease in T_c attributed to the Θ_D reduction with lattice expansion.

2.2.1 Phonon softening and Transition temperature (T_c) reduction with lattice expansion

T_c variation with the lattice expansion $\Delta a = a - a_0$, where $a_0 (= 3.3\text{\AA})$ [20] is the lattice parameter for the bulk Nb with $T_c = 9.2$ K. From the BCS theory[22], the superconducting temperature (T_c) is given by

$$k_B T_c = 1.13 \hbar \omega_D \exp\left[-\frac{1}{N(0)V}\right] \quad (2.2.1)$$

where k_B is the Boltzman constant, \hbar the reduced Plancks constants, ω_D is the Debye frequency, $N(0)$ is the density of state (DOS) at the fermi level (E_F), and V is the pairing potential.

ω_D is related to the Debye temperature (Θ_D) by $\hbar \omega_D = k_B \Theta_D$. From this relationship $T_c \propto \omega_D$ provided that there is no change in $N(0)$ and V . Since $\omega_D \propto \sqrt{K}$, where K is the force constant due to the interatomic interactions between the neighboring atoms, we can write as,

$T_c \propto \omega_D \propto \sqrt{K}$. The relation between the lattice parameter and the force constant(k) is given by the second derivative of the interatomic potential ($\phi(r)$). Thus for unexpanded lattice ($r = r_0$),

$$k = k(0) = \phi'(r_0) \quad (2.2.2)$$

In the presence of a stress field at the grain boundary the lattice expand and the

No.	t (nm)	D (nm)	a (Å)	ρ (10 K) ($\mu\Omega$ cm)	ℓ (nm)	T_c (K)	ΔT_c (K)
1	18.0	6.0	3.51	216.4	0.18	-	-
2	22.0	5.6	3.52	262.5	0.14	-	-
3	24.0	7.3	3.49	149.5	0.25	-	-
4	29.0	8.5	3.47	140.8	0.26	-	-
5	61.0	8.7	3.41	120.7	0.30	4.7	0.9
6	117.0	7.0	3.36	97.3	0.38	6.2	0.4
7	148.5	7.2	3.36	92.6	0.40	6.2	0.4
8	185.0	8.3	3.35	75.9	0.49	6.4	0.3
9	372.5	10.2	3.33	50.5	0.74	7.7	0.2

Figure 2.2: A summary of various sample parameters for different niobium thin films[20]

separation between neighboring atoms changes from r_0 to $r_0 + \Delta r$. Thus, the stress field is expressed as a small linear perturbation modifying $\phi(r)$ to $\phi_1(r) = \phi(r) + \epsilon r$ where ϵ is proportional to the stress (strain). The modified force constant is given by $k(\Delta r) = \phi'(r_0 + \Delta r)$.

Choosing an appropriate interatomic potential (the Morse potential) to find a relationship between the lattice expansion and k or eventually T_c . The interatomic potential for transition metals with cubic structure is given by

$$\phi(r) = B[\exp(-2C(r - r_0)) - \exp(-C(r - r_0))] \quad (2.2.3)$$

with B and C are constants with dimensions of energy and inverse of length and r_0 is the equilibrium separation between the nearest neighbors. By taking the second derivative of the $\phi(r)$ at $r = r_0 + \Delta r$ we get the new spring constant as a function

of Δr as,

$$K(\Delta r) = K(0)[2\exp(-2C\Delta r) - \exp(-C\Delta r)] \quad (2.2.4)$$

where $K(0) = 2C^2B$ is the spring constant with no lattice expansion. Nb is a bcc metal and thus $\Delta r = \frac{\sqrt{3}}{2}\Delta a$. The T_c variation with lattice expansion is then given by ,

$$T_c(\Delta a) = T_c(0)[2\exp(-1.732C\Delta a) - \exp(-0.866C\Delta a)]^{1/2} \quad (2.2.5)$$

provided that there is no change in $N(0)$ and V with the lattice expansion. Here, $T_c(0)$ is the T_c for $\Delta a = 0$. fig. 2.3 The graph shows the decrease in T_c with lattice expansion for the characteristic length scale $1/C = 0.25 \text{ \AA}$ and $T_c = 9.2\text{K}$ for Nb.

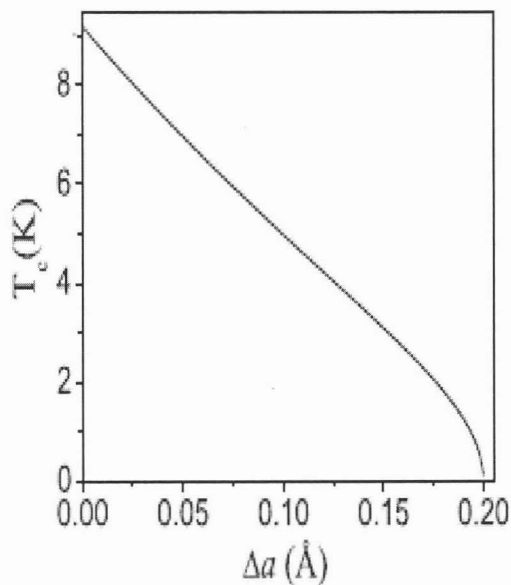


Figure 2.3: Variation of T_c with lattice expansion (Δa) [20]

2.3 Temperature and Energy gap in superconducting Niobium

The energy gap is one of the key characteristics of the superconducting state of materials. It is used when electrons at the Fermi level are considered. The energy gap at zero temperature (Δ) in the weak coupling limit [22] can be evaluated as:

$$\Delta(0) = 2\hbar\omega_D \exp\left(\frac{-1}{N(0)V}\right) \quad (2.3.1)$$

where ω_D is the Debye frequency, $N(0)$ is the density of single-electron states of a given spin orientation at the Fermi level and V is the electron lattice interaction potential. The energy gap (Δ) at any temperature is given by

$$\Delta(T) = 3.06K_B T_c \sqrt{1 - \frac{T}{T_c}} \quad (2.3.2)$$

The BCS theory estimates the energy gap at zero temperature ($\Delta(0)$) as

$$\Delta(0) = 1.76K_B T_c \quad (2.3.3)$$

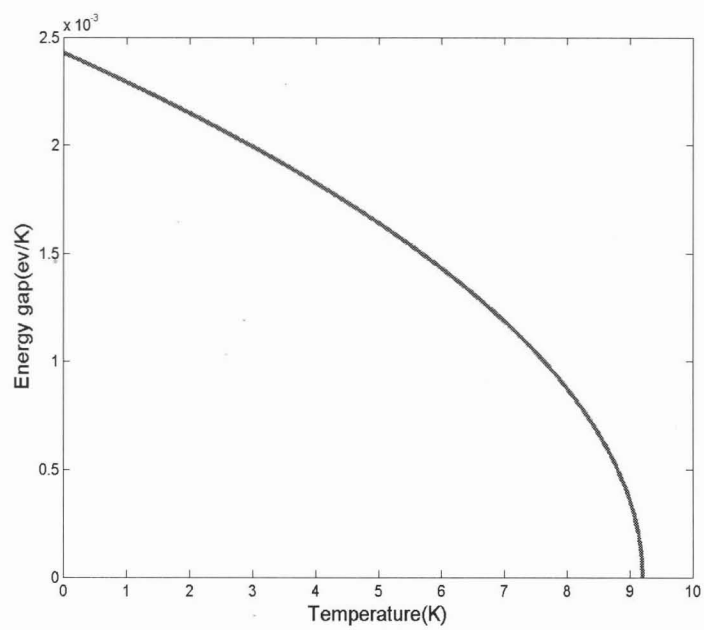


Figure 2.4: Energy gap vs temperature for bulk Nb

The energy gap is the order parameter for the superconductor, with a phase factor given by $e^{i\phi}$.

Hence, the order parameter is equal to $\Delta e^{i\phi}$. The Quasiparticle excitations above the BCS ground state are coherent superpositions of the electron and hole quasiparticles and are in one-to one correspondence with excitations in the normal state. Adding one quasiparticle to the BCS ground state adds energy E to the system given by:

$$E = \sqrt{\left(\frac{\hbar^2 K^2}{2m - E_F}\right)^2 + \Delta^2}$$

where, k is the quasiparticle momentum.

The corresponding quasiparticle density of states (DOS) is represented by

$$N(E) = N(0) \frac{E}{\sqrt{E^2 - \Delta^2}}$$

where, $N(0)$ is the normal state DOS and E is the energy of the quasiparticle.

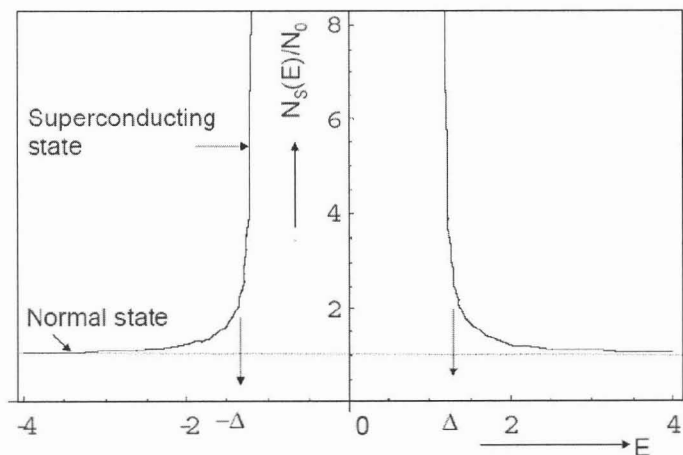


Figure 2.5: DOS as a function of energy relative to the Fermi energy at the Fermi level[26]

2.4 Superconductivity and Size

The enhanced interest of the researchers in nanoparticles is due to the discovery of unusual physical and chemical properties which are related to manifestation of the so-called quantum size effects. From the energy stand-point, a decrease in the particle size results in an increase in the fraction of the surface energy in its chemical potential[23]. A nanoparticle is a quasi-zero-dimensional nano-object in which all characteristic linear dimensions are of the same order of magnitude (not more than 100 nm). Nanoparticles can basically differ in their properties from larger particles, for example, from long- and well-known ultradispersed powders with a grain size above 0.5 μm . As a rule, nanoparticles are shaped like spheroids. Nanoparticles with a clearly ordered arrangement of atoms (or ions) are called nanocrystallites. Nanoparticles with a clear-cut discontinuity of the system of electronic energy levels are often referred to as 'quantum dots' or 'artificial atoms' (most often, they have compositions of typical semiconductor materials).

A fundamental problem in nanoscience research is to provide a conceptual description of the nature of the ground state in confined systems. In particular, despite several decades of active research[24], understanding of the modification of superconductivity at reduced length scales is yet to be achieved. Changes in superconducting properties may be expected when the effective size of a superconductor is reduced below its characteristic length scales, such as the London penetration depth $\lambda_L(T)$ or the coherence length $\xi(T)$. Since long range order cannot persist down to the zero dimensional limit, it is interesting to probe how superconducting properties evolve below these length scales. A complete destabilization of superconducting order is expected when the system size is so small that the electronic level spacing becomes larger than

the bulk superconducting energy gap (Δ). Thus, the so-called Anderson criterion suggests that, in principle, superconductivity may persist at length scales much below the coherence length (ξ). The critical temperature (T_c) and the superconducting energy gap Δ change with decreasing particle size in sputter-deposited nanostructured. For Nb ($\Delta \approx 1.6\text{meV}$) and $\xi \approx 3.8\text{nm}$, the electron-phonon coupling strength $\frac{2\Delta}{k_B T_c} \approx 3.9$ [25]. A direct correlation between the measured values of (Δ) and T_c in nano niobium. Nb, which was found to remain in the intermediate coupling BCS regime down to 8 nm. Thus, the evolution of superconductivity with particle size in Nb is quite distinct from that in other weak and strong coupling superconductors. Understanding of the modification of superconductivity at reduced length scales is yet to be achieved. Changes in superconducting properties may be expected when the effective size of a superconductor is reduced below its characteristic length scales, such as the London penetration depth (λ_L) and the coherence length (ξ). Since long range order cannot persist down to the zero dimensional limit, it is interesting to probe how superconducting properties evolve below these length scales. A complete destabilization of superconducting order is expected when the system size is so small that the electronic level spacing becomes larger than the bulk superconducting energy gap (Δ).

2.5 Size effects on the normal and superconducting properties of Niobium

It is important to know the ground state properties of a superconductor when its effective dimensions become less than the characteristic length scales, such as the

penetration depth (λ_L) and the coherence length (ξ). There are many studies of superconducting systems at reduced scale, such as thin films[24], nanowires and granular materials. Superconductivity is known to persist at dimensions lower than ξ and λ_L . In 1959, Anderson obtained that there is a third length scale that controls the superconducting order parameter in nano superconductors. According to the Anderson criterion, there will be complete destabilization of superconductivity for grain sizes at which the energy level spacing (arising from quantum size effects in small particles) becomes equal to the superconducting energy gap, $\Delta(0)$. This criterion has been experimentally verified in many elemental superconductors. However, the mechanism of controlling the variation of the superconducting T_c with size has remained debatable. There are two alternative mechanisms to explain the variation of the superconducting transition temperature in finite size superconductors. According to the first mechanism, the changes in T_c occur due to surface effects caused by a reduction in the phonon frequencies (phonon softening) arising from the larger surface to volume ratio in nanoparticles. The second mechanism for the size dependence of T_c is related to quantum size effects arising from the quantization of the electronic wave vector (k). With decreasing grain size, there is a discretization of the energy levels which can decrease the effective density of states. According to the BCS relation, this would result in a decrease in T_c with decreasing size. However, it should be noted that this mechanism will cause a proportionate effect on T_c and $\Delta(0)$. Thus, a complete understanding of the mechanism influencing T_c in nanosuperconductors requires one to determine the size dependence of the electron-phonon coupling constant (λ). The understanding of superconductivity at reduced length scales cannot be complete without a detailed study of T_c , $\Delta(0)$ and H_c at nano scales. It should be noted that the

superconducting properties like T_c , $\Delta(0)$ and the critical fields (H_c) are interrelated parameters. Their correlation between the nanosize, the superconducting energy gap and the critical temperature T_c is investigated theoretically and experimentally. By systematically reducing the characteristic size of the superconductors and nanocells the crossover between the bulk superconducting regime and fluctuation-dominated superconductivity regime will be revealed. The theoretical values are obtained based on the solution of the GinzburgLandau (GL) equations with the realistic boundary conditions imposed through nanostructuring. Superconducting proximity effect in nanocomposites and nano-grains embedded in a normal metal or superconducting matrix forms yet another interesting problem in nanosuperconductivity. According to the theory of superconducting proximity, when a superconductor is in close proximity with a normal metal or another superconductor with a lower T_c , then the superconducting wave function may penetrate across the interface into the normal metal and a pair-breaking effect on the Cooper pairs is felt in the superconducting side. This phenomenon is observed when the thickness of the normal metal and the superconductor are both less than their respective coherence lengths. The coherence length of most elemental superconductors ranges between few tens of nm to a few hundred nm. Superconductivity in nano-sized materials has been a subject of extensive studies because of its pure physical interests and possible application toward quantum switch and quantum computers. In particular, vortices in superconductors whose lateral size are in the same order as the coherence length have attracted lots of attention since several unique configurations of the vortices have been reported, such as giant vortex and anti-vortex, depending on its size and shape.

Currently, unique physical properties of nanoparticles are under intensive research

special place belongs to the magnetic properties in which the difference between a massive (bulk) material and a nanomaterial is especially pronounced. In particular it was shown that, magnetization (per atom) and the magnetic anisotropy of nanoparticles can be much greater than those of a bulk specimen, while differences in the Curie (T_c) or Neel (T_N) temperatures, i.e., the temperatures of spontaneous parallel or antiparallel orientation of spins, between nanoparticle and the corresponding microscopic phases reach hundreds of degrees. In addition, magnetic nanomaterials were found to possess a number of unusual properties in giant magnetoresistance, abnormally high magnetocaloric effect, and so on.

2.6 Previous studies on nanosize Niobium

Nanoscale superconductivity has been studied over the past three decades. It is important to know how the ground state properties change when one or more of the system dimensions are reduced below the characteristic length scales for a bulk superconductor: the coherence length and the London penetration depth[26]. The superconducting properties for confined systems often show dramatic changes from those of the bulk. At much reduced dimensions, new phenomena not seen in bulk superconductors may also be observed in Nanoscale superconductivity. The decrease in T_c in Nb is attributed mainly to the changes in the density of states at the Fermi level with decreasing grain size.

The thermal conductivity of the metal is an important criterion, which determines the thermal stability of the superconductor. The thermal conductivity of pure niobium at temperatures lower than 9.2 K is given by the theory of metals, modified in order to take into account the superconducting state. The thermal conductivity of a metal

is dominated by that of the electron gas, but the lattice heat conductivity due to the propagation of phonons, has to be added. This can be written as:

$$K = K_e + K_L$$

The electron heat conduction in the superconducting state is reduced because the electrons which have condensed into Cooper pairs do not contribute to any disorder or entropy transport any more. The remaining fraction of electrons do contribute to heat transport, but this decreases very rapidly with decreasing temperature. This decrease in electron heat conduction can be calculated using the BCS theory, when the thermal resistance is mainly due to impurity scattering[27] In nanocrystalline Nb films, the superconducting T_c decreases with a reduction in the average particle size below 20nm. The decrease in T_c with a reduction in the superconducting energy gap measured by point contact spectroscopy. Consistent with the Anderson criterion, no superconducting transition was observed for sizes below 8 nm. It is shown that the size-dependence of the superconducting properties in the intermediate coupling Type II superconductor is governed by changes in the electronic density of states rather than by phonon softening.

Despite several decades of active research, a satisfactory understanding of the modification of superconductivity at reduced length scales is yet to be achieved. Changes in superconducting properties are expected when the effective size of the superconductor is reduced below its characteristic length scales, such as the London penetration depth and coherence length Since long-range order cannot persist down to the zero dimensional limit. It is interesting to probe how the superconducting properties evolve below these length scales. A complete destabilization of superconducting order is

expected when the system size is so small that the electronic level spacing becomes larger than the bulk superconducting energy gap (Δ). Thus, the so-called Anderson criterion, suggests that, in principle, superconductivity may persist at length scales far below coherence length ξ . The evolution of T_c and the superconducting energy gap (Δ) with decreasing particle size in nanocrystalline thin films of Nb is investigated by S. Bose and et al[28]. For Nb, the value of the electron-phonon coupling strength, ($2\Delta/k_B T_c \sim 3.8$, falls between ($2\Delta/k_B T_c \sim 3.6$) and ($2/k_B T_c \sim 4.5$). The experiments were performed on nanocrystalline thin films with average grain sizes (D) in the 5nm-50nm range, synthesized by high pressure magnetron sputtering. All films with $D > 20nm$ show bulk superconductivity with $T_c = 9.2K$, while there is a gradual suppression of T_c between 20nm and 8nm. No superconducting transition was detected for $D < 8nm$, consistent with the Anderson criterion. Clearly, there is no size-dependent enhancement in T_c in nano-Nb. Finally, we demonstrate a direct correlation between the measured values of Δ and T_c in nano-Nb, which was found to remain in the weak coupling BCS regime down to the lowest particle size studied. This suggests that, the evolution of superconducting properties with particle size in Nb is distinct from the other weak and strong coupling superconductors studied so far. the energy bands of a bulk solid split into discrete levels with a reduction in size, physical properties of nanoparticles show marked differences from those of bulk materials. Size dependent changes in structural, electronic, and magnetic properties have been observed in many metals.

Nanostructural materials have become attractive because of their unique characteristics that can hardly be obtained from conventional bulk materials owing to their quantum size and surface effects. So, there has been considerable interest in fabrication

of low-dimensional nanosized materials such as nanowires, nanorods and nanotubes because they possess distinctive geometries, novel physical and chemical properties, and have potential applications in nanodevices and find diverse applications in nanotechnology.

2.7 Upper critical field in nanostructured Nb

The upper critical field in nanometer-sized Nb particles is governed by the changes in the effective Ginzburg-Landau coherence length (λ_{GL}) occurring due to two competing factors: (i) the decrease in the grain size and (ii) the effective decrease in the density of states at the Fermi level due to the formation of a Kubo gap[26]. As a result, the upper critical field (H_{C2}) in nanostructured Nb shows non-monotonic grain size dependences. Between 60nm to 20nm, H_{C2} is found to increase by 2.5 times while there is no appreciable decrease in the superconducting transition temperature (T_C) from its bulk value of 9.2K. This causes a decrease in the coherence length (ξ_{GL}) due to a reduction in the mean free path with decreasing size. Below 20 nm, however, H_{C2} decreases with decreasing size. In this size range, there also occurs a decrease in the T_C as well as the superconducting energy gap(Δ). The decrease in H_{C2} in this regime causes the decrease in the density of states at the Fermi level due to a quantization in the electronic energy levels[30].

The upper critical field (H_{C2}) in Type-II superconductors is given by

$$H_{c2}(T = 0) = 0.69T_c \frac{4ecK_B}{\hbar} N(0)\rho_N$$

where e is the electronic charge, $N(0)$ is the density of states at the Fermi level ,

K_B is the Boltzmann constant and ρ_N is the normal state resistivity.

H_{c2} can be related to the ξ_{GL} as,

$$H_{c2}(T) = \frac{\phi_0}{2\pi \left[\xi_{GL}(T) \right]^2} \text{ where } \phi_0 \text{ is the flux quantum given by } \phi_0 = \frac{h}{2e}.$$

The intrinsic coherence length (ξ_{GL}) is given by

$$\xi_{GL}(T) = 0.85 \frac{\left(\xi_0 L_{eff} \right)^{1/2}}{\left[1 - \frac{T}{T_c} \right]^{1/2}}$$

where L_{eff} is the mean free path, ξ_0 is the intrinsic coherence length,

$$H_{c2} = \frac{\phi_0}{2\pi \xi_{GL}^2}$$

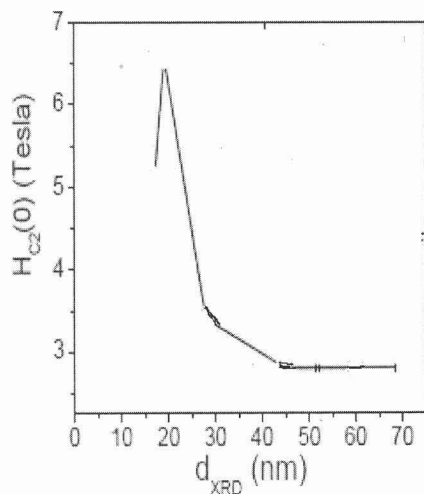


Figure 2.6: Variation of H_{C2} with grain size for the nano-Nb[26]

$\xi_0 = \frac{0.18\hbar V_F}{K_B T_c}$ and V_F is the fermi velocity. For Nb H_{C2} increases from its bulk value of 2.8 T for the film with the largest grain size (60nm) that shows the bulk T_C to 6.9T for the film with a grain size 19nm with $T_C = 7.8K$. However, for the films with

grain size below 19nm, H_{C2} decreases till it reaches a value of 5T for the smallest sized superconducting sample[26].

Chapter 3

Mathematical formulation

In this chapter we will show the relationship between transition temperature (T_c), the electron-phonon coupling parameter (λ) and the Coulomb's pseudopotential (μ^*) using the coupling theory and also we will evaluate the energy gap using the Gips free energy model.

3.1 Transition temperature of strong-coupled superconductors

The electron-phonon interaction is still the most generally accepted mechanism for the occurrence of superconductivity. In this part we will calculate the transition temperature using the so-called "strong-coupling" theory, as a function of the coupling constants for the electron-phonon and Coulomb's interactions. To do this we will write down the integral equations for the strong-coupled superconductor at the transition temperature.

According to the BCS theory, the relationship between the transition temperature

(T_c), typical phonon energy ($\langle\omega\rangle$) and the interaction strength ($N(0)V$) is given by

$$T_c = 1.14\langle\omega\rangle \exp\left[\frac{-1}{N(0)V}\right] \quad (3.1.1)$$

$N(0)$ is the electronic density of states at the fermi surface and V is the pairing potential arising from the electron-phonon interaction. However, the weak coupling BCS equations for T_C are thus no longer valid in the nanostructured system. In the strong coupling limit, T_C is given by the McMillans equation[29].

The integral equation for the normal and pairing self energies at the transition temperature are given by:

$$\begin{aligned} \xi(\omega) &= \left[1 - z(\omega)\right] \omega \\ &= \int_0^{\omega_q} d\omega' \int_0^{\omega_0} d\omega_q \alpha^2(\omega_q) F(\omega_q) \\ &\times \left\{ [N(\omega_q) + f(-\omega')] [(\omega' + \omega_q + \omega)^{-1} + (\omega' + \omega_q - \omega)^{-1}] - [N(\omega_q) + f(\omega)] \right. \\ &\quad \left. [(-\omega' + \omega_q + \omega)^{-1} - (-\omega' + \omega_q - \omega)^{-1}] \right\} \end{aligned} \quad (3.1.2)$$

$$\begin{aligned} \Delta(\omega) &= [z(\omega)]^{-1} \int_0^{\infty} \frac{d\omega'}{\omega'} \\ &\times R_e[\Delta(\omega')] \int_0^{\omega_0} d\omega_q \alpha^2(\omega_q) F(\omega_q) \\ &\times \left\{ [N(\omega_q) + f(-\omega')] [(\omega' + \omega_q + \omega)^{-1} + (\omega' + \omega_q - \omega)^{-1}] - [N(\omega_q) + f(\omega')] \right\} \end{aligned}$$

$$\left[(-\omega' + \omega_q + \omega)^{-1} + (-\omega' + \omega_q - \omega)^{-1} \right] \left\} - \frac{N(0)V_c}{z(\omega)} \right. \\ \left. \int_0^{E_B} \frac{d\omega'}{\omega'} \times R_e[\Delta(\omega')][1 - 2f(\omega')] \right. \quad (3.1.3)$$

where $f(\omega)$ is the phonon density of state, ω_0 is the maximum phonon frequency, $\alpha^2(\omega_q)$ is the average electron-phonon interaction, V_c the matrix element of the screened coulomb's interaction averaged over the fermi surface, E_B the electronic band width, $N(\omega)$ and $f(\omega)$ the Bose and fermi occupation probabilities $[\exp(\frac{\omega}{K_B T_c}) \mp 1]^{-1}$. we can obtain the approximate solution of eq.(3.1.2) by substituting a trial function for $\Delta(\omega)$ on the right hand side of eq.(3.1.2) and computing the given integration. However, it is required that the trial function for $\Delta(\omega)$ and the computed $\Delta(\omega)$ should be consistent.

Now take,

$$\Delta_t(\omega) = \Delta_0 \quad \text{for} \quad 0 < \omega < \omega_0 \quad (3.1.4)$$

$$\Delta_t(\omega) = \Delta_\infty \quad \text{for} \quad \omega_0 < \omega \quad (3.1.5)$$

$\omega(0)$ and $\Delta(\infty)$ can be computed from eqs.(3.1.2 and 3.1.3)

If we ignore the thermal phonons, there will have three different contributions to $\Delta(0)$. The first contribution is given by :

$$\Delta'(0) = [Z(0)]^{-1} \int_0^{\omega_0} \frac{d\omega'}{\omega'} \Delta(0) \int_0^{\omega_0} d\omega_q \alpha^2(\omega_q) F(\omega_q) \times \left\{ f(-\omega')(\omega' + \omega_q)^{-1} - f(\omega')(-\omega' + \omega_q)^{-1} \right\} \\ \cong \left(\frac{\Delta_0}{Z(0)} \int_0^{\omega_0} \frac{d\omega'}{\omega'} \tanh \left(\frac{\omega'}{2T_c} \right) \right) 2 \int_0^{\omega_0} \frac{d\omega_q \alpha^2(\omega_q) F(\omega_q)}{\omega_q}$$

$$\Delta'(0) \cong \left[\frac{\Delta_0 \lambda}{z(0)} \right] \ln \left(\frac{\omega_0}{T_c} \right) \quad (3.1.6)$$

The dominant contribution to the ω' integral is for small ω' and we neglect it relative to ω_q in the phonon propagators $(\omega' + \omega_q)^{-1}$. The dimensionless electron-phonon coupling constant (λ) is given

$$\lambda = 2 \int_0^{\omega_0} \alpha^2(\omega) F(\omega_q) \frac{d\omega_q}{\omega_q} \quad (3.1.7)$$

This parameter roughly corresponds to the density of state at the fermi level ($N(0)V$) of the BCS theory.

The second contribution is $\Delta''(0)$ given by

$$\begin{aligned} \Delta''(0) &= [Z(0)]^{-1} \int_{\omega_0}^{\infty} \frac{d\omega'}{\omega'} \Delta_{\infty} \int_0^{\omega_0} d\omega_q \alpha^2(\omega_q) F(\omega_q) \frac{2}{\omega_q + \omega'} \\ &\cong \left[\Delta_{\infty} / z(0) \right] \left(\langle \omega \rangle \lambda / \omega_0 \right) \end{aligned} \quad (3.1.8)$$

where $\langle \omega \rangle$ is the average phonon frequency.

$$\langle \omega \rangle = \frac{\int_0^{\omega_0} d\omega_q \alpha^2(\omega_q) F(\omega_q)}{\int_0^{\omega_0} \frac{d\omega_q}{\omega_q} \alpha^2(\omega_q) F(\omega_q)} \quad (3.1.9)$$

$$\cong 0.5\omega_0 \quad (3.1.10)$$

The third contribution is $\Delta'''(0)$ given by

$$\Delta'''(0) = \left[\frac{N(0)V_c}{z(0)} \right] \times \left[\Delta_0 \ln \left(\frac{\omega_0}{T_c} \right) \right] + \Delta_{\infty} \ln \left(\frac{E_B}{\omega_0} \right) \quad (3.1.11)$$

The first two contributions (i.e $\Delta'(0)$ and $\Delta''(0)$) are obtained from the electron-phonon interactions and the third contribution (i.e $\Delta'''(0)$) is from the Coulomb's

interaction. At high energies, the only contribution is from Coulomb's interaction:

$$\Delta(\infty) = \left[N(0)V_c/Z(\infty) \right] \left[\Delta_0 \ln(\omega_0/T_c) + \Delta_\infty \ln(E_B/\omega_0) \right] \quad (3.1.12)$$

From the expressions given above the value of the re-normalization is found to be

$$z(0) = 1 + \lambda$$

$$z(\infty) = 1$$

To satisfy our consistency at high and low energies

$$\Delta(0) = \Delta_0 = \Delta'(0) + \Delta''(0) + \Delta'''(0) \quad (3.1.13)$$

$$\Delta(0) = \left[\frac{\Delta_0}{z(0)} \right] \ln\left(\frac{\omega_0}{T_c}\right) + \left[\frac{\Delta_\infty}{z(0)} \right] \left(\frac{\langle \omega \rangle}{\omega_0} \right) \lambda - \left[\frac{N(0)V_c}{z(0)} \right] \left[\Delta_0 \ln\left(\frac{\omega_0}{T_c}\right) + \Delta \ln\left(\frac{E_B}{\omega_0}\right) \right] \quad (3.1.14)$$

and also

$$\Delta(\infty) = \Delta_\infty \quad (3.1.15)$$

$$\Delta(\infty) = -N(0)V_c \left[\Delta_0 \ln\left(\frac{\omega_0}{T_c}\right) + \Delta_\infty \ln\left(\frac{E_B}{\omega_0}\right) \right] \quad (3.1.16)$$

$$\Delta(\infty) = -\frac{N(0)V_c \Delta_0 \ln\left(\frac{\omega_0}{T_c}\right)}{1 + N(0)V_c \ln\left(\frac{E_B}{\omega_0}\right)} \quad (3.1.17)$$

$$\Delta(\infty) = -\mu^* \Delta_0 \ln\left(\frac{\omega_0}{T_c}\right) \quad (3.1.18)$$

where μ^* is the Coulomb's pseudopotential given by

$$\mu^* = \frac{N(0)V_c}{1 + N(0)V_c \ln\left(\frac{E_B}{\omega_0}\right)} \quad (3.1.19)$$

$$= -\mu^* \Delta_0 \ln\left(\frac{\omega_0}{T_c}\right) \quad (3.1.20)$$

Now, inserting eq.(3.1.18) in to eq.(3.1.14) we get

$$\Delta_0 = \frac{\Delta_0 \left[\lambda - \mu^* - \mu^* \lambda \left(\frac{\langle \omega \rangle}{\omega_0} \right) \right] \ln\left(\frac{\omega_0}{T_c}\right)}{1 + \lambda} \quad (3.1.21)$$

Finally solving for T_c , we get

$$\frac{T_c}{\omega_0} = \exp\left(\frac{-(1 + \lambda)}{\lambda - \mu^* - \left(\frac{\langle \omega \rangle}{\omega_0}\right) \lambda \mu^*}\right) \quad (3.1.22)$$

$$T_c = \omega_0 \exp\left(\frac{-(1 + \lambda)}{\lambda - \mu^* - \left(\frac{\langle \omega \rangle}{\omega_0}\right) \lambda \mu^*}\right) \quad (3.1.23)$$

For weak coupling, $\lambda \ll 1$. In a weak coupling, eq.(3.1.23) reduces to the BCS result with $\lambda - \mu^*$ plays the role of $N(0)V$ where as in strong coupling, the interactions are renormalized by $z = 1 + \lambda$ and the Coulomb's interaction changes the gap function in such a way that the phonon contribution is changed from λ to $\lambda[1 - \left(\frac{\langle \omega \rangle}{\omega_0}\right) \mu^*]$

The energy gap function $\Delta(\omega)$ for a typical set of parameters, $\lambda = 0.91$, $\mu^* = 0.149$ and $T_c = 10K$ corresponds roughly to Nb[29]. In order to find a more accurate solution for the gap equation, we use a simple iterative procedure, the gap equation (3.1.3) can be written in a form

$$\Delta_{n+1}(\omega) = \int d\omega' K(\omega, \omega') \Delta'_n \quad (3.1.24)$$

Now, choosing $\Delta_1(\omega)$ and substitute on the right hand side of eq(3.1.23). and perform the indicated integration to find $\Delta_2(\omega)$ which is of course closer to the true solution. After successive eight iterations, $\Delta(\omega)$ converges to third decimal place. During the iteration it is convenient to fix T_c and the Coulomb's pseudopotential(μ^*) and we need to adjust α^2 at each stage so that $\Delta_{n+1}(0) = \Delta_n(0)$.

Again we must choose a particular parameter $\alpha^2(\omega_q)F(\omega_q)$ because $F(\omega_q)$ is the phonon density of state of Nb and found from neutral work. $\alpha^2(\omega_q)$ is taken to be constant and we take $\alpha^2 F(\omega) = 0$ for strong coupling. The value of μ^* lies between

0 and 0.2. If $\mu^* = 0$, eq.(3.1.23) becomes

$$T_c = \omega_0 \exp\left(\frac{-(1 + \lambda)}{\lambda}\right) \quad (3.1.25)$$

.In order to determine the constant $\frac{\langle \omega \rangle}{\omega_0}$, we introduce a new parameter y given by

$$y = \left(\lambda - \frac{1.04(1 + \lambda)}{\ln(\Theta/1.45T_c)} \right) / \mu^* \quad (3.1.26)$$

3.1.1 Determination of λ using The phonon frequencies

Now, take,

$$\alpha^2(\omega)F(\omega) = \frac{\int_s \frac{d^2p}{v_F} \int_s \frac{d^2p'}{(2\hbar\pi)^3 v_{F'}} \sum_v g_{pp'} v^2 \delta(\omega - \omega_{p-p'} v)}{\int_{s'} \frac{d^2p}{v_F}} \quad (3.1.27)$$

where the integral $\int d^2p$ is taken over the fermi surface and the electron-phonon matrix element is given by

$$g_{pp'} v = \left[\frac{\hbar}{2MNV \omega_{p-p'} v} \right]^{1/2} \wp_v(p, p') \quad (3.1.28)$$

where $\wp_v(pp')$ is the electronic matrix element of the change in the crystal potential (v) as one atom is removed.

$$\wp_v(pp') = \int \Psi_{p'}^* (\varepsilon_{p-p'} v \cdot \nabla v) \Psi_p d\tau \quad (3.1.29)$$

Note that, g^2 is inversely proportional to the phonon energy $\omega_{p-p'}$, so that the first moment of $\alpha^2(\omega)F(\omega)$ is independent of the phonon frequency.

Thus,

$$\int_0^\infty d\omega \omega \alpha^2(\omega)F(\omega) = \frac{\int \frac{d^2p}{v_F} \int \frac{d^2p'}{(2\pi)^3 v_{F'}} \sum \frac{\hbar}{2MNV} \wp_v^2(pp')}{\int \frac{d^2p}{v_F}}$$

$$= \frac{N(0)\hbar\langle\wp^2\rangle}{2M} \quad (3.1.30)$$

Here, $\langle\wp^2\rangle$ is the average over the fermi surface of the square of the electronic matrix element. Finally from the definition of λ we have,

$$\lambda = 2 \int_0^\omega \alpha^2(\omega) F(\omega) \frac{d\omega}{\omega}$$

$$\lambda = \frac{N(0)\langle\wp^2\rangle}{M\langle\omega^2\rangle} \quad (3.1.31)$$

where $\langle\omega^2\rangle$ is the average of the square of the phonon frequency and M is the isotopic mass.

The transition temperature also depends on isotopic mass directly through the factor Θ and implicitly through ω_0 which depends on μ^* .

$T_c \sim M^\alpha$ with the isotopic shift α . Where α is given by;

$$\alpha = 1/2 \left(1 - \frac{(1+\lambda)(1+0.62\lambda)\mu^{*2}}{[\lambda - \mu^*(1+0.62\lambda)]^2} \right)$$

$$= 1/2 \left[1 - \left(\mu^* \ln \frac{\Theta}{1.45T_c} \right)^2 \frac{1+0.62\lambda}{1+\lambda} \right] \quad (3.1.32)$$

3.2 Ginzburg-Landau Theory, Free energy expansion

Some of the key ideas for the Landau mean field description of phase transitions were developed in the context of superconductivity[30].

For a complex order parameter Ψ the Landau expansion of the free energy for small Ψ would be,

$$F = \int \left[\alpha(T)|\Psi|^2 + \frac{1}{2}\beta(T)|\Psi|^4 + \gamma(T)|\nabla\Psi|^2 \right] d^3x \quad (3.2.1)$$

where Ψ is the complex wave function of the superconductor that fulfils the role of the order parameter.

For a charged superfluid we must add the coupling to the vector potential and also the magnetic energy, so that the full expression for a pair-superconductor is given by:

$$F = \int \left[\alpha(T)|\Psi|^2 + \frac{1}{2}\beta(T)|\Psi|^4 + \gamma(T)|(\nabla + \frac{2ie}{\hbar c}A)\Psi|^2 + \frac{B^2}{8\Pi} \right] d^3x \quad (3.2.2)$$

where A is the vector electromagnetic field potential.

Near the transition temperature (T_c), $\alpha(T) \rightarrow a(T - T_c)$, $\beta \rightarrow b$, considering a, b and γ independent of temperature. The free energy F must be minimized with respect to variations of Ψ and A . Minimizing F with respect to A gives,

$$\frac{\delta F}{\delta A} = 0 = \frac{-2e\gamma}{\hbar} i \left[\Psi^\dagger (\nabla + \frac{2ie}{\hbar c}A)\Psi - \Psi (\nabla - \frac{2ie}{\hbar c}A)\Psi^\dagger + \frac{1}{4\Pi} \nabla \times (\nabla \times A) \right] \quad (3.2.3)$$

$$\nabla \times B = \frac{4\Pi}{c} j \text{ with } j = \frac{4e}{\hbar} \gamma |\Psi|^2 (\Delta\phi + \frac{2e}{\hbar c}A)$$

The above expressions give the London penetration depth

$$\frac{1}{\lambda^2} = 32\Pi \left(\frac{e^2}{\hbar^2 c^2} \right) \gamma |\Psi|^2 \quad \text{and} \quad \gamma |\Psi|^2 = n_s \frac{\hbar^2}{8m} \quad (3.2.4)$$

since only the product parameters $|\Psi|^2$ and γ are needed,

$$|\Psi|^2 = \frac{1}{n_s} \text{ and } \gamma = \frac{\hbar^2}{4m} \quad (3.2.5)$$

Then

$$j = -\frac{e\hbar}{m} |\Psi|^2 \left(\Delta\phi + \frac{2e}{\hbar c} A \right) \quad (3.2.6)$$

The results shows that, near T_c the superfluid density varies as,

$$n_s \propto \left(1 - \frac{T}{T_c}\right)$$

Minimizing the free energy with respect to Ψ^\dagger gives:

$$\frac{\delta F}{\delta \Psi^\dagger} = 0 = \alpha(T)\Psi + \beta(T)|\Psi|^2\Psi - \gamma(T)\left[\nabla + \frac{2ie}{\hbar c}A\right]^2\Psi \quad (3.2.7)$$

Using the convention in equation (3.2.5) equation (3.2.7) can be written in a form that makes an analogy to the Schrodinger equation for particles of mass $2m$.

Thus

$$\frac{1}{4m}(-i\hbar\nabla + \frac{2e}{c}A)^2\Psi + \alpha(T)\Psi + \beta(T)\Psi^2\Psi = 0 \quad (3.2.8)$$

Although this is a convenience for solving the equation, rather than anything deep, because n_s is a stiffness constant and it is more natural to normalize the order parameter in terms of the strength of long range correlations.

Near the transition temperature equation (T_c), eq.(3.2.7) becomes

$$-a(T - T_c)\Psi + b|\Psi|^2\Psi - \gamma\left(\nabla + \frac{2ie}{\hbar c}A\right)^2\Psi = 0 \quad (3.2.9)$$

The solution of equation (3.2.8) for a normal state is given by,

$$|\Psi|^2 = \frac{a(T_c - T)}{b} \quad (3.2.10)$$

, yielding the usual square root growth of the order parameter for $T < T_c$ found in mean field theories.

The free energy density for $T < T_c$ is given by,

$$f = \frac{F}{V} = -\frac{a^2(T - T_c)^2}{2b} \quad (3.2.11)$$

yielding the jump in the specific heat at T_c by two differentiations with respect to temperature. The zero temperature energy would be approximated as,

$$F(T \simeq T_c) \sim -N \frac{(K_B T_c)^2}{\varepsilon_F} \left(1 - \frac{T}{T_c}\right)^2 \quad (3.2.12)$$

so that

$$\frac{a^2}{b^2} \sim \frac{nK_B^2}{\varepsilon_F} \quad (3.2.13)$$

For spatial variations of the order parameter in Eq. (3.29) yields the length scale ξ given by

$$\xi^2 = \frac{\gamma}{\alpha} = \frac{\gamma}{a}(T_c - T)^{-1} \quad \text{or} \quad \xi = \xi_0 \left(1 - \frac{T}{T_c}\right)^{-\frac{1}{2}} \quad (3.2.14)$$

with the temperature independent length scale $\xi_0 = \frac{\gamma}{a}T_c$. On the other hand from eq.(3.2.4) $\gamma|\Psi|^2 = n_s \frac{\hbar^2}{8m}$ approximating n_s (at $T \rightarrow 0$) as n ,

$$\gamma \frac{a}{b} T_c \sim n \frac{\hbar^2}{2m} \quad (3.2.15)$$

so that

$$\xi_0^2 \sim \frac{\hbar^2}{2m\varepsilon_F} \left(\frac{\varepsilon_F}{K_B T_c}\right)^2 \quad (3.2.16)$$

The coherence length is therefore a factor $\frac{\varepsilon_F}{K_B T_c}$ larger than $\left(\frac{\hbar^2}{2m\varepsilon_F}\right)^2$ which is the order of the interparticle spacing. This can be traced to the fact that the stiffness constant is determined by the total density of electrons, whereas the energy coefficients a , b are given by the fraction of particles corresponding to the energy band of width about $K_B T_c$ around the Fermi surface that is affected by the pairing. The Ginzburg criterion for the temperature T_G near T_c when fluctuations become important can be estimated as $f\xi^3 \sim K_B T_c$. With the above results, this is estimated as $1 - \frac{T_G}{T_c} = t_G$.

Thus we get,

$$\frac{n(K_B T_c)^2}{\varepsilon_F} t_G^{\frac{1}{2}} \left[\frac{\hbar^2}{2m\varepsilon_F} \left(\frac{\varepsilon_F}{K_B T_c}\right)^2 \right]^{\frac{3}{2}} \sim K_B T_c \quad (3.2.17)$$

$t_G \sim \frac{K_B T_c}{\varepsilon_F}$ This is very small for conventional (low temperature) superconductors, so that fluctuation corrections and the critical region near T_c are usually immeasurable.

In a constant imposed magnetic field H (i.e. the field due to external current sources) the appropriate free energy is given by,

$$G_H = F - B(x) \cdot H / \Pi \quad (3.2.18)$$

In the normal state $B(x) = H$, whereas in the bulk superconducting state $B = 0$. Thus the simplest idea would be that superconductivity is destroyed at a thermodynamic critical field H_c given by:

$$\frac{H_c^2}{8\Pi} = \frac{\alpha^2}{2\beta} \quad (3.2.19)$$

For fields larger than this, the system becomes normal. This would be disappointing, since for typical superconductors this critical field would be only a few hundred gauss even at low temperatures. To proceed, it is useful to simplify the Ginzburg-Landau equation by introducing the London penetration depth (λ). Taking magnetic fields $\sqrt{2}H_c$, the order parameter $|\alpha|/\beta$ and the energy density $\frac{H_c}{4\Pi}$. Then the free energy density is given by:

$$f = -|\Psi^2| + \frac{1}{2}|\Psi|^4 + \left| (iK^{-1}\nabla + A)\Psi \right|^2 + B^2 \quad (3.2.20)$$

With

$$\kappa = \frac{\lambda}{\xi_L} \quad (3.2.21)$$

$$\kappa = \frac{1}{4} \left(\frac{\hbar c}{e\gamma} \right) \left(\frac{\beta}{2\Pi} \right)^2 \quad (3.2.22)$$

Although λ depends strongly on temperature, this mainly cancels out in the ratio, and κ is roughly temperature independent. It is the key parameter in determining the nature of the behavior in a magnetic field. The value of κ varies from small to

large values in different superconductors.

In the dimensionless units the Ginzburg-Landau equation is given as:

$$(-i\kappa^{-1}\nabla + A)^2\Psi - \Psi + |\Psi|^2\Psi = 0 \quad (3.2.23)$$

In modern notation the expression of the electron-phonon coupling parameter is expressed as,

$$\lambda = 2 \int dw \frac{\alpha^2(\omega)F(\omega)}{\omega} \quad (3.2.24)$$

where $F(\omega)$ is the density of the phonon states in energy and $\alpha^2(\omega)$ is the square of the electron-phonon coupling constant averaged over polarization directions of phonons. Note that, λ is always positive so that the fermi surface is stable if the lattice is stable. Values of λ for various metals range from 0.5 to 1.5. The parameter corresponds roughly to the $N(0)V$ phonon of the BCS theory.

3.3 Transition temperature and phonon-coupling in Nb

The most extensive study of the relation between superconducting transition temperature (T_c) superconducting-coupling limit (λ) is made by McMillan[31]

$$\mu = N_t(o)|V_c| \quad (3.3.1)$$

where $N_t(o)$ is the single-spin density of the electron phonon spectral function $\alpha^2F(\omega)$ defined as

$$\alpha^2F(\omega) = N_t(o) \frac{\sum_{kk'} |M_{kk'}|^2 \delta(\omega - \omega_Q) \delta(\epsilon_k) \delta(\epsilon_{k'})}{\sum_{kk'} \delta(\epsilon_k) \delta(\epsilon_{k'})} \quad (3.3.2)$$

where $\vec{Q} = \vec{K} - \vec{K}'$, ω_Q and ϵ_k are phonon and electron energies respectively, Q and k run over wave number and quantum number for phonons and electrons and $M_{kk'}$ is the electron-phonon coupling matrix element and δ functions restrict the electrons to the fermi surface. The zero- temperature Eliashberg theory determines the complex energy -gap function $\Delta(\omega)$, and the finite-temperature. Eliashberg theory helps to determine the critical temperature T_c . The quantity $|\Delta(\omega)|^2$ can be measured by quasiparticle tunneling. The finite-temperature Eliashberg theory relates T_c to a small number of simple parameters:

$$T_c = \frac{\langle \omega \rangle}{1.2} \exp\left(-\frac{1.04(1 + \lambda)}{\lambda - \mu^*(1 + 0.62\lambda)}\right) \quad (3.3.3)$$

The original McMillan equation contains $\frac{\Theta}{1.45}$ instead of $\frac{\langle \omega \rangle}{1.2}$ which was introduced later by dynes. The parameter λ is a dimensionless measure of the strength of α^2F :

$$\lambda = 2 \int d\omega \frac{\alpha^2 F}{\omega} \quad (3.3.4)$$

The quantity $1+\lambda$ plays the role of an electron mass enhancement and renormalizes certain observables such as electron specific heat. In the BCS theory, λ corresponds to $N_t(0)|V_{ph}|$. The parameter μ^* is an effective Coulomb's repulsion reduced from instantaneous repulsion μ by the fact that Coulomb's coupling is propagated more rapidly than phonon coupling.

$$\frac{1}{\mu^*} = \frac{1}{\mu} + \ln\left(\frac{\omega_{el}}{\omega_{ph}}\right) \quad (3.3.5)$$

The ratio $\frac{\omega_{el}}{\omega_{ph}}$ is ratio of propagation times. ω_{el} is the plasma frequency and ω_{ph} is the cut off high-frequency. A time lag occurs in the electron pairing which is the source of both the frequency dependance of $\Delta(\omega)$ and the reduction of the effective Coulomb's repulsion. $\langle \omega \rangle$ is the first moment of the normalized weight function

$$g(\omega) = (2/\lambda\omega)\alpha^2 F(\omega)$$

$$\langle \omega^n \rangle = \frac{2}{\lambda} \int d\omega \alpha^2 F(\omega) \omega^{n-1} \quad (3.3.6)$$

The value of T_c can be determined from the interaction parameters $\alpha^2 F(\omega)$ and μ^* via the Eliashberg equation. The solution of $\Delta(\omega)$ resembles to the measured gap equation at low temperatures.

The Matsubara representation of the gap equation is given by:

$$\rho \bar{\Delta}(i\omega_n) = \Sigma(\lambda(n - m) - \mu) \quad (3.3.7)$$

3.4 Anderson criteria

According to this criterion, when the discrete energy level spacing (δ) in nanoparticles becomes equal to the superconducting energy gap (Δ) superconductivity can no longer be sustained in the small particle. In a bulk superconductor, electrons present in the energy interval Δ from the Fermi level condense to form the BCS state, thereby opening up an energy gap $\sim \Delta$ at the Fermi level. However, for small particles, when $\Delta \sim \delta$, there are no available electrons within the energy interval Δ of the Fermi level to form the condensate state and hence the superconducting state cannot be stabilized. The critical particle size for the disappearance of superconductivity can be calculated from the Anderson criterion as follows.

For a nanoparticle of diameter D , the energy level spacing (Kubo gap)[32] is given by:

$$\delta = \frac{4\epsilon_F}{3N} \quad (3.4.1)$$

where, N is the total number of conduction electrons in the particle given by $N = \frac{D}{\lambda_F^3}$.
 λ_F is the fermi wavelength.

Therefore

$$\delta = \frac{4\epsilon_F \lambda_F^3}{3D^3} \quad (3.4.2)$$

And the energy gap in terms of the clean limit coherence length is given as,

$$\Delta = \frac{0.18\hbar v_F}{\xi_0} \quad (3.4.3)$$

Chapter 4

Results and Discussions

This chapter focuses on the analysis of the inter-relationship that exist among superconducting transition temperature (T_c), the electron-phonon coupling constant (λ) and the interaction Coulomb's pseudopotential (μ^*) for nanosized Nb using the equations obtained in the previous chapter. Here we will present a theoretical argument and empirical evidence using graphs.

From eq.(3.1.24) we have,

$$T_c = \omega_0 \exp\left(\frac{-(1 + \lambda)}{\lambda}\right) \quad (4.0.1)$$

Substituting ω_0 by the Debye temperature Θ we get,

$$T_c = \Theta \exp\left(\frac{-(1 + \lambda)}{\lambda}\right)$$

As can be seen from fig.4.1, the transition temperature varies exponentially with the parameter $(1 + \lambda/\lambda)$. As λ decreases T_c also decreases.

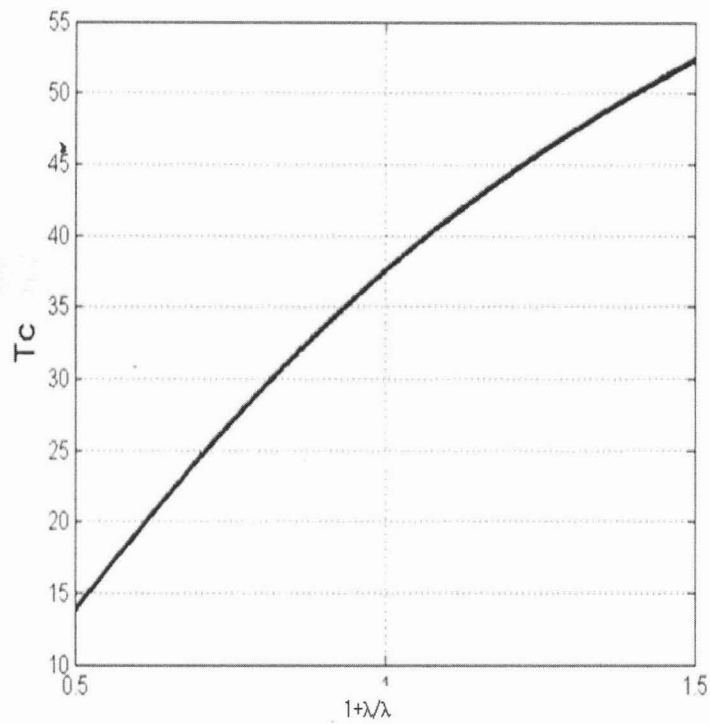


Figure 4.1: variation of critical temperature with the parameter $(1 + \lambda/\lambda)$ for $\mu^* = 0$

Similarly, From eq.(3.1.25) if $\mu^* = 0$

$$\ln\left(\frac{\Theta}{T_c}\right) = \frac{1 + \lambda}{\lambda} \quad (4.0.2)$$

As can be seen from fig.4.2, $\ln(\Theta/T_c)$ varies linearly with $\frac{1+\lambda}{\lambda}$. The superconducting

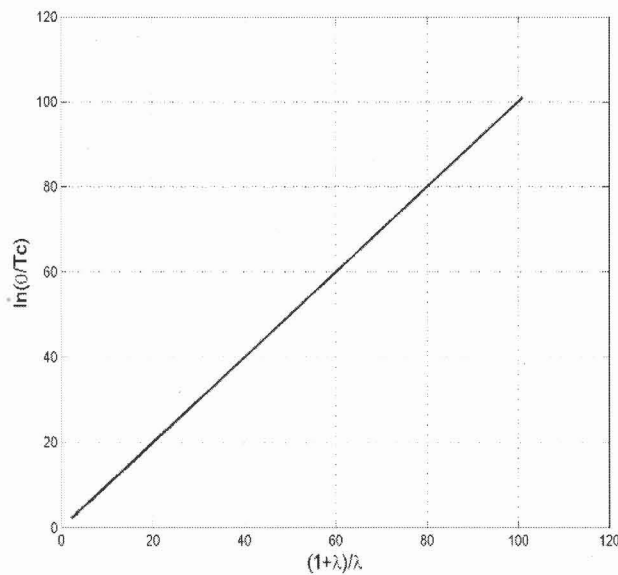


Figure 4.2: graph of $\ln\left(\frac{\Theta}{T_c}\right)$ vs $\frac{1+\lambda}{\lambda}$

temperature (T_c) of Nb decreases as the coupling constant (λ) decreases with a decrease in particle size.

The graph of $\ln\frac{\Theta}{T_c}$ versus $\frac{1+\lambda}{\lambda}$ for $\mu^* = 0$ is a straight line with slope 1.04 and an intercept of 0.37 which is equal to $\ln 1.45$.

From the previous equation(eq.3.1.26) we have introduced a parameter y given by

$$y = \left(\lambda - \frac{1.04(1 + \lambda)}{\ln(\Theta/1.45T_c)} \right) / \mu^* \quad (4.0.3)$$

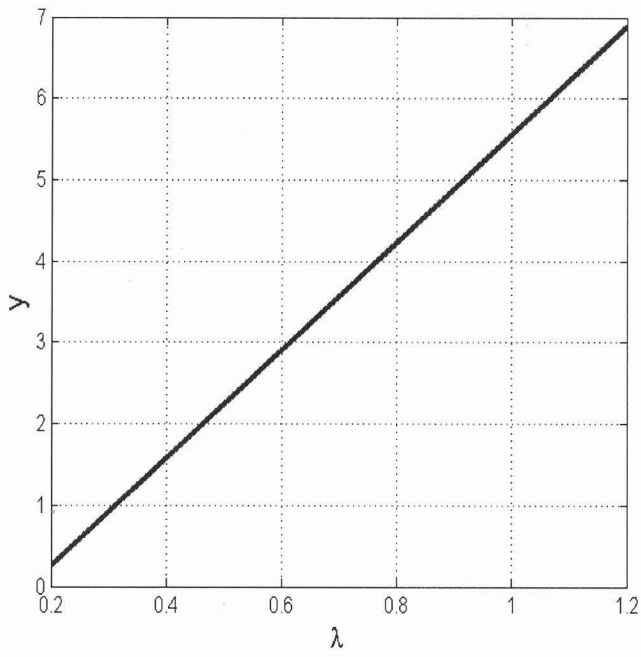


Figure 4.3: The parameter y vs λ graph for $\mu^* = 0.13$

The graph of y vs λ is a straight line similar in form with the graph of $1 + \left(\frac{\langle\omega\rangle}{\omega_0}\right)\lambda$ versus λ a straight line graph with slope $\frac{\langle\omega\rangle}{\omega_0} = 0.62$ and an intercept of 1. We have used Θ for the characteristic phonon frequency. For Nb, $\Theta = 277^0k$, $\omega_0 = 330^0k$ and $\langle\omega\rangle = 230^0k$.

The final Modified McMillan formula for the transition temperature is then given by,

$$T_c = \frac{\Theta}{1.45} \exp \left[- \frac{(1.04 + \lambda)}{\lambda - \mu^*(1 + 0.62\lambda)} \right] \quad (4.0.4)$$

From the Mcmillan's equation it is clear that surface effects may cause T_c to increase or decrease with decreasing particle size depending on how fast λ increases with respect to μ^* . With decreasing particle size, increasing disorder leads to an increase in the repulsive interaction between the electrons as screening effects decreases. Therefore if λ increases faster than μ^* , T_c increases significantly.

$$\mu^* = \frac{0.26N(E_F)}{1 + N(E_F)}. \quad (4.0.5)$$

McMillan showed that λ is approximately proportional to the inverse of the average squared phonon frequency $\langle\omega^2\rangle$. Thus, a reduction in $\langle\omega^2\rangle$ should lead to an increase in λ . It is clear from McMillan's equation that a higher coupling strength (due to size reduction) produce higher T_C .

Again As can be observed from fig.4.4 the transition temperature change linearly with the electron-phonon coupling constant(λ)

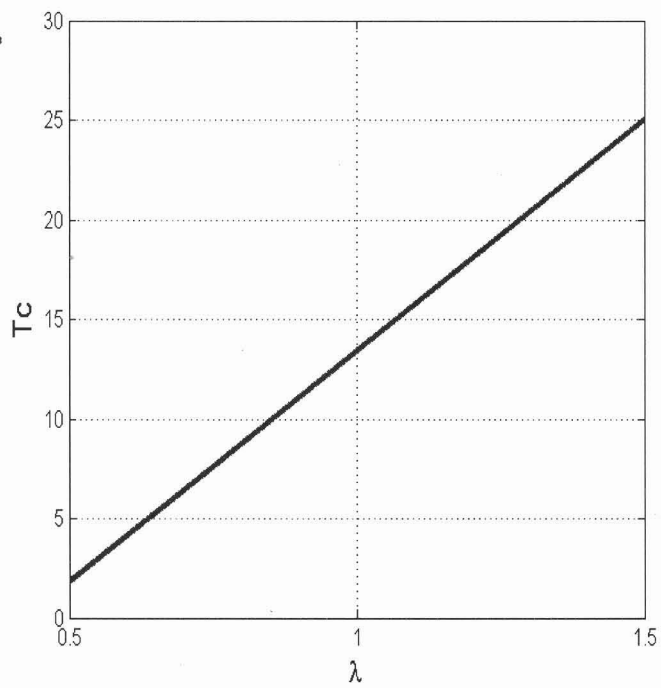


Figure 4.4: T_c vs λ graph for $\mu^* = 0$

Chapter 5

Conclusions and Recommendations

The superconductivity property of materials in general and Niobium in particular depend on particle size. The characteristic parameters like energy gap, coherence length, transition temperature and electron-phonon coupling constant in nanosized materials are completely different from the bulk materials.

The transition temperature and energy gap of Niobium (Nb) depends highly on particle size which also affects electron-phonon coupling parameter and the Coulomb's pseudopotential. From the relations we obtained, the critical temperature (T_c) depends exponentially with the coupling constant (λ) and the Coulomb's pseudopotential (μ^*). The decrease in critical temperature is generally attributed to the decrease in coupling constant for insignificant variation of the Coulomb's pseudopotential.

Finally we recommended that since nanosized Nb is applicable for different purposes: for the fabrication of magnetic resonance imaging (MRI), superconducting quantum interference devices (SQUIDS), Radio frequency (RF) cavities and others, further and intensive experimental studies should be conducted on various properties of nanosized Nb.

Bibliography

- [1] H.K.Onnes, Akad.Vanwetenschappen(amsterdam), **14**, 113(1911).
- [2] Teaching and learning package, University of cambridge, sep.2008.
- [3] C. Kittel, introduction to solid state physics, 8th ed.
- [4] W.Meissner and R.Ochsenfeld, Naturwiss, **21**, 787(1933).
- [5] Werner Buckel, Reinhold Kleiner, superconductivity: fundamentals and applications, second edition, WILEY-VCH verlag, 2004.
- [6] A. Abrikosov, Sov.phys., JETP, **5**, 1174(1957).
- [7] Mark A. Roseman, PhD thesis, study of superconducting niobium films, McGill University Montreal, Canada, October 2011.
- [8] Robert W.Dull, a teacher guide to superconductivity for high school students, Largo high school, Largo Florida, 1993.
- [9] J.Barden, L.N.Copper and J.R Schrieffer, phys.Rev. **108**, 1175(1957).
- [10] J.G. Bendorz, K.A. Mueller, Z. Phys.Rev. B, **64**, 189(1986).

- [11] P. Lebrum, Cryogenesis for the large hadron collider, *IEEE transactions on applied superconductivity*, **10**, 1(2000).
- [12] Ulrich. H. Winenand, the SSC low energy booster, *IEEE*, 1997.
- [13] Ziad Melhem, superconducting materials and applications, oxford instruments nanoscience, UK.
- [14] Andrei Mourachkine, room temperature superconductivity, university of Cambridge, UK.
- [15] Deborah Elcock, Potential impacts of nano technology on energy transmission applications and needs, Nov.2007.
- [16] Surinder Mann, Nanotechnology and construction, Institute of nanotechnology, 2006.
- [17] Monica McCoy, Nanotechnology in construction: Nano materials and devices offer macro improvements in concrete materials, 2005.
- [18] Warren DeSorbo, Effect of dissolved gases on some superconducting properties of niobium, October 1963.
- [19] H.P. Roeser, D.T. Haslam et al, Correlation between transition temperature and crystal structure of niobium, vanadium, tantalum and mercury superconductors, *Acta Astronautica C* **67**, 1333(2010).
- [20] Dibyendu Hazra , Mintu Mondal, Anjan K. Gupta, Correlation between structural and superconducting properties of nano-granular disordered Nb thin films, *Physica C.*, **469** , 268(2009).

- [21] S. Bose et al., Phys. Rev. Lett. 95 (2005).
- [22] M. Tinkham, Introduction to Superconductivity, second ed., McGraw-Hill, New York, 1996.
- [23] Sangita Bose, et al , Competing effects of surface phonon softening and quantum size effects on the superconducting properties of nanostructured Nb, Phys. Condens. Matter **21** , 2009.
- [24] Sangita Bose, et al, Mechanism of the Size Dependence of the Superconducting Transition of Nanostructured Nb, **95**, (2005).
- [25] Sangita Bose, et al, Size dependence of the Tc and the superconducting energy gap in nanocrystalline thin films of Nb, The Ohio State University, Columbus.
- [26] S. Bose, PhD thesis, Size Effects in Nanostructured Superconductors, Tata Institute of Fundamental Research, Mumbai.
- [27] Parametrization of the niobium thermal conductivity in the superconducting state, Supercond. Sci. Technol. 9(1996), UK.
- [28] Sangita Bose, Pratap Raychaudhuri, Rajarshi Banerjee and Pushan Ayyub, Upper critical field in nanostructured Nb: Competing effects of the reduction in density of states and the mean free path, Tata Institute of Fundamental Research, India.
- [29] W.L. McMillan, Transition temperature of strong-coupled superconductors, Physical Review Letters, **167** , 331(1967).

- [30] M.R. Beasley, Santa Barbara, Notes on the Ginzburg-Landau Theory, ICMR Summer School on Novel Superconductors, University of California, August 2009.
- [31] P.B.Allen, transition temperature of strong-coupled superconductors reanalyzed, *phys.rev B*, **12**, 905(1975).
- [32] S. Bose, et al, Size induced metal insulator transition in nano structured Nb thin films, institute of fundamental research, Mumbai, 2005.

Declaration

I, hereby declare that this thesis is my original work and has not been presented for a degree in any other university, and that all sources of materials have been duly acknowledged.

Name: Yilak Seyoum

Signature: 

Date: June 21

This thesis has been submitted for the examination with my approval as a University advisor.

Name: Dr.Geberegziabher Kahasay

Signature : 

Date: 21 June 2012